NICOLAUS COPERNICUS UNIVERSITY IN TORUŃ

Bulletin of Geography. Physical Geography Series, No. 29 (2025): 43–63
http://doi.org/10.12775/bgeo-2025-0009

Morphometry-based flood hazard zonation of Ajay River basin using coupled TOPSIS–VIKOR models, India

Shanku Ghosh[1*][a], **Chakkaravarthi Prakasam**[2]

[1]Assam University Diphu Campus (A Central University), Department of Geography, School of Earth Sciences, Diphu, Karbi Anglong, Assam, India

[2]Assam University, Department of Geography, School of Earth Sciences, Diphu Campus, Diphu, Assam, India

*Correspondence e-mail: cprakasam@gmail.com

[a]https://orcid.org/0009-0009-6613-0354; [b]https://orcid.org/0000-0003-0515-4714

Abstract. The main aim of the study is to delineate flood-hazard-prone zones in the Ajay River basin using advanced multi-criterion decision-making (MCDM) models. TOPSIS and VIKOR are the two models which were employed, due to their complex decision-making ability and efficient integration of multiple influencing factors. The Ajay River is a severely flood-prone river; flooding of the river is concentrated within the monsoon season, triggered by successive episodes of the high-intensity monsoonal precipitation that inundates the lower floodplain. Post-independence, the river has experienced several flood events, which continue to constitute a major issue in the lower floodplain of the river. Fourteen flood conditioning factors, i.e. drainage density, drainage texture, drainage frequency, Normalized Difference Water Index (NDWI), confluence density, soil type, geology, elevation, relief, dissection index, ruggedness, slope, length of overland flow and infiltration number, were used to generate the final flood hazard maps. Parameter weightages were calculated using the Analytic Hierarchy Process (AHP). The two models showed very similar results; while the TOPSIS model classified 8% and 24% of the basin area as highly and very highly hazard-prone, respectively, the VIKOR model assigned 10% and 23% of the basin area to the same respective classes. These areas are spread throughout the floodplains of the lower Ajay River basin. The validation flood points were obtained from the annual flood report of West Bengal (2023). The Receiver Operating Characteristics (ROC) curve method was used, and both models revealed high accuracy, with area under the ROC curve (AUC) values of 0.827 and 0.837. These results confirm the models' suitability for similar environmental conditions, making them valuable tools for strategic flood-hazard management planning in the study area.

Key words:
MCDM,
Geomorphic Analysis,
AHP,
Flood Hazard Mapping

Introduction

Global flood risk is a growing concern, with studies indicating a worldwide increase because of climate change (Glas et al. 2019; Duan et al. 2022; Prasojo et al. 2024). Flood occurrence is governed by complex meteorological and environmental factors, making its complete prevention infeasible. Therefore, it is crucial to get better at predicting floods and finding ways to lessen their impact. This will help in minimizing damage and casualties. An important initial step in flood risk assessment is to map areas more likely to flood. This can identify vulnerable zones and support the planning of measures to minimize potential losses (Khosravi et al. 2019). Overall, flood hazard mapping methods are classified into three categories, namely physical-

based, physical, and empirical modeling. The physical-based models include conceptual physical-based modeling and data-driven hydrological models, whereas empirical models include machine-learning, statistical and multi-criterion decision-making (MCDM) models. There was a 35% increase in applications of empirical MCDM methods in flood hazard modeling between 2000 and 2020 (Mudashiru et al. 2021). Empirical MCDM models help analyze and manage flood risk by providing a structured way to evaluate options based on different criteria. They aid decision-making and support efficient flood management plans (Negese et al. 2022). The MCDM models are frequently used for flood hazard, vulnerability and risk assessment, flash flood mapping, and flood prediction (Debnath et al. 2023), due to their ability to deal with multiple, often contrasting criteria and handle complex decision-making (Bedada and Dibaba 2025). The AHP is a subjective MCDM model that is mostly used for flood mapping (Gupta and Dixit 2022; Kader et al. 2024; Vashist and Singh 2024; Zhran et al. 2024); other MCDM models that are extensively used are TOPSIS, MOORA, WASPAS, EDAS, VIKOR and DEMATEL.

Floods are the single largest disaster type, accounting for 21% of total disaster deaths, 13.46% of injuries, 46.73% of the disaster-affected population, and 24.38% of global disaster economic damage (Antwi-Agyakwa et al. 2023). Asia is home to 73% of the global flood-risk-prone population. Within Asia, South Asia is most affected (39% of the continent's flood-affected population), followed by Southeast Asia (30%) and East Asia (20%) (Di Baldassarre et al. 2010). India ranks as the world's second most flood-affected country, after China (Gupta and Dixit 2022).

The Indian climate features monsoon rainfall. With numerous rivers, prolonged heavy rainfall often leads to widespread flooding. According to the Central Water Commission (CWC 2010), approximately 40 million hectares of Indian land are flood-prone. Out of this, an annual average of 7.6 million hectares undergo inundation. CWC data reveal that floods caused approximately $200 billion in capital losses and 92,000 deaths between 1953 and 2009 (CWC 2010; Sarkar and Mondal 2019). Flood damage varies across Indian states; Bihar, West Bengal, Odisha, Assam, Andhra Pradesh and Gujarat are particularly vulnerable (Sheth et al. 2022). In 2018, Kerala experienced severe floods with extensive damage to property, infrastructure and agriculture, requiring approximately Rs. 30 billion for rebuilding (Devanand and Kundapura 2020). Maharashtra, especially districts like Mumbai, Palghar, Thane, Raigad, Satara, Sangli, Pune and Kolhapur, experienced significant flooding in 2019 due to heavy rainfall, highlighting the need for mitigation and adaptation strategies (Mishra et al. 2024). Ten Indian states account for 46% of the country's flood impact. Among these, Uttar Pradesh and Bihar are most affected; 55% of Bihar's geographical area is flood-prone, followed by Assam (50%), Uttar Pradesh (37%) and West Bengal (32%).

West Bengal is flood-prone across 42.43% of its area (37,660 km²); with the exception of five years, the state underwent flood inundation every year from 1960 to 2000. Within the same time period, the state underwent flood inundation covering between 5,000 and 10,000 km² on ten occasions, and four times inundation exceeded 20,000 km². Because of the differential nature of rivers, the flood problem in the state varies among different regions like North Bengal, Rarh region and the delta region. Rivers like the Bramhni, Mayurakshi, Ajay and Damodar are spread over the Rarh region of West Bengal; after originating from the Jharkhand plateau, they pass through the Rarh region and have their confluence in the Bhagirathi-Hooghly River. These rivers generate floods due to their non-perennial character and their associated limited carrying capacity being exceeded by runoff from high-intensity monsoonal rainfall (Irrigation & Waterways Department). The lower Ajay River basin is one of the frequently flood-affected areas of west Bengal. Floods have occurred in the river basin at various times, viz. 1956, 1959, 1970, 1971, 1973, 1978, 1984, 1995, 1999, 2000, 2006 and 2007. Over the years, the flood-affected area of the basin has been increasing in size, as has the frequency of occurrence. In the year 1956, 680.70 km² of the basin was flood-affected, whereas in 2000 this increased to 1488.85 km², simultaneously increasing the flood-induced sand-splay issue. (Mukhopadhyay 2010; Roy 2023). The flood issue has been addressed in studies conducted by Mukerji et al. (2009), Mukhopadhyay (2010), Bandyopadhyay et al. (2016), Roy (2020), Chandra et al. (2023), Roy (2023) and Ghosh and Prakasam (2024). Flooding remains a significant problem in the study area, necessitating researchers' attention to address the issue further. Limited studies have addressed the geomorphic, topographic and drainage characteristics of the

 Citation: Bulletin of Geography. Physical Geography Series 2025, 29, http://doi.org/10.12775/bgeo-2025-0009

study area and its influence on flood occurrence. This article attempts to study the flood problem of the Ajay River basin using different geomorphic, topographic and drainage parameters and assigns weights to these parameters using knowledge-based subjective AHP and a rank-based TOPSIS–VIKOR model to generate a final flood-hazard map that delineates the study area into different flood-hazard zones. MCDM models were applied due to their systematic integration of a range of datasets and flexible data incorporation, which prioritize these models over the hydrologic and hydraulic approaches in potential hazard zonation. TOPSIS is a decision-making tool that ranks options by their closeness to an ideal solution and distance from a negative-ideal solution. The best option is closest to the ideal and furthest from the negative ideal, determined by calculating each option's distance from the ideal. VIKOR identifies ideal-best and -worst solutions to find a compromise (Sah and Pan 2024; Thakkar and Thakkar 2021).

Study area

The basin extends between 23°24′27′′N and 24°36′14′′N latitude and 86°16′13′′E and 88° 10′1′′E longitude (Fig. 1). The river originates at 320 meters above mean sea level near Saraun village in the Chakai Community Development block of Bihar, following a flow path of 299 km from source to confluence. After entering West Bengal at Simjuri, near Chittaranjan, it flows for 152 km through densely populated districts before merging with the Bhagirathi-Hooghly River at Katwa. The basin spans three states in eastern India, namely West Bengal (Birbhum, Purba Bardhhaman districts and Paschim Bardhhaman), Jharkhand (Deoghar Jamtara and Giridih) and Bihar (Jamui district). For most of its course, it serves as a natural boundary between Bardhhaman (Paschim and Purba) and Birbhum districts in West Bengal. The Paharo, Kunur, Hinglow, Jayanti, Kander, Tumuni and Darhwa are the major tributary rivers of Ajay

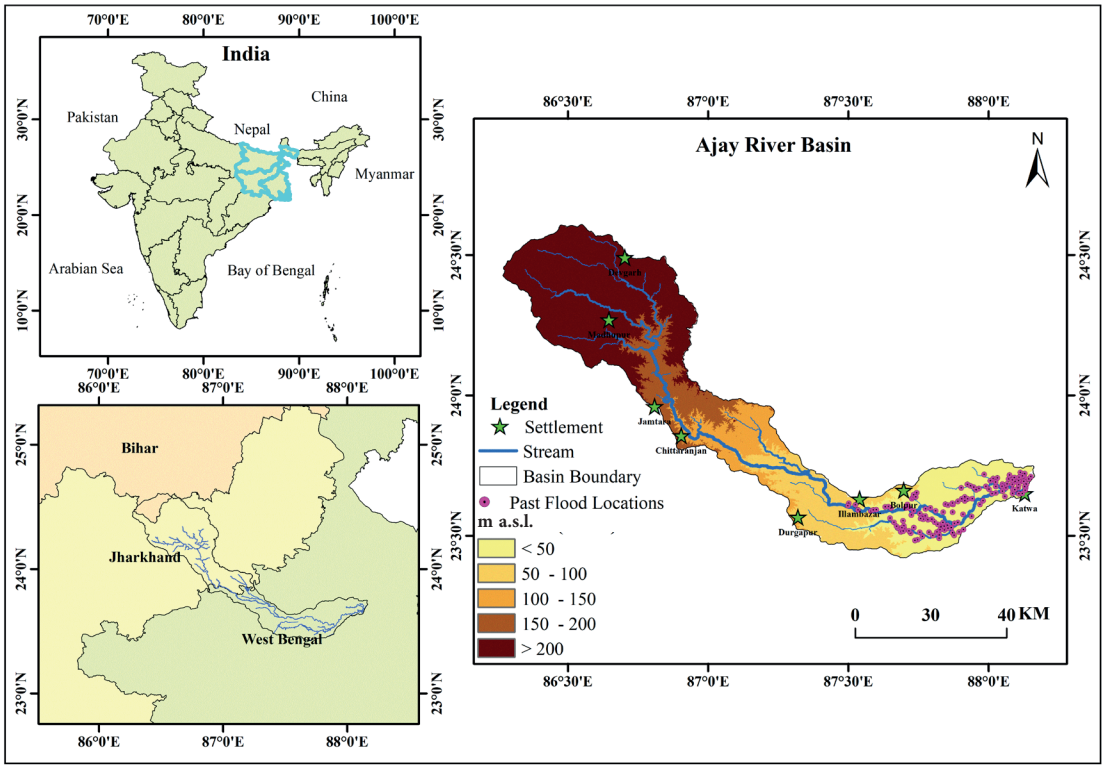

Fig. 1. Study Area map of Ajay River basin

River. The upper (northern) boundary of the basin is defined by the Mayurakshi river system, while the Damodar River basin defines the lower (southern) boundary in West Bengal, and both of them are major river system of West Bengal.

Methodology

According to the methodological flowchart (Fig. 2), the study used two MCDM techniques to generate the final flood hazard map (FHM) by integrating fourteen flood-conditioning factors. All the thematic layers were reclassified in the GIS framework using the equal-interval method, where the cell values are divided into equally sized classes. The generated maps were validated using the Area Under the Receiver Operating Characteristic Curve (AUC–ROC) method.

Flood-Conditioning Factors and Flood Inventory Map

Flood risk is influenced by numerous factors, and there is no single standard for choosing Flood Conditioning Factors (FCFs). Because risk is a complex, multi-dimensional concept encompassing hazard, vulnerability and exposure,

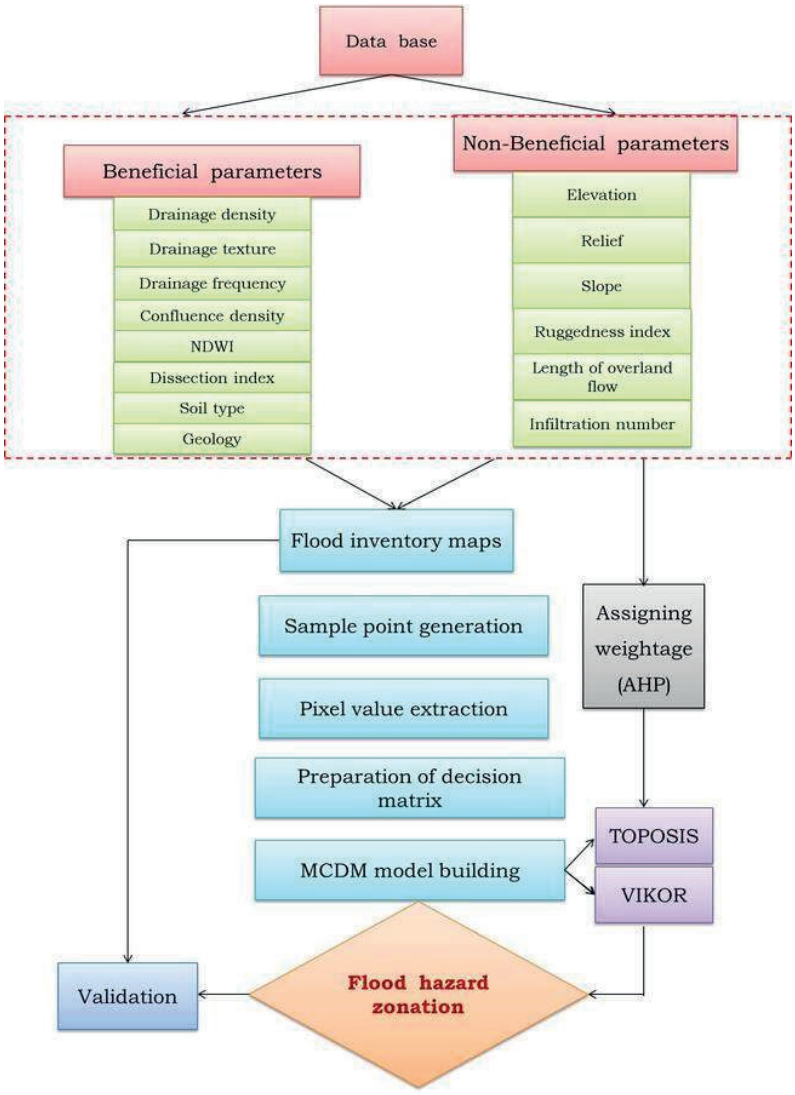

Fig. 2. Methodological flowchart of the study

Citation: Bulletin of Geography. Physical Geography Series 2025, 29, http://doi.org/10.12775/bgeo-2025-0009

FCFs must be carefully selected to represent all aspects of flood risk (Shah and Pan 2024). In this study, fourteen flood-influencing factors (Fig. 3) were selected – namely, drainage density, length of overland flow, drainage frequency, infiltration number, confluence density, relief, drainage texture, elevation, roughness, slope, geology, Normalized Difference Water Index (NDWI) and soil type. The parameters were selected considering the previous flood-related studies in the study area, researcher knowledge and the geomorphic characteristics of the study area. The influencing factors were further reclassified into five classes of equal pixel size. Further based on functional characteristics and flood-inducing capacity, the conditioning factors were classified into non-beneficial and beneficial categories (Table 1).

The layers – namely, absolute reliefs, relative reliefs, ruggedness number, and slope – were extracted from ASTER DEM at a 30-meter spatial resolution. The drainage parameters were extracted from Survey of India (SOI) topographical maps having RF 1:50,000. The study area soil-type data were collected from NBSS & LUP; geological data were collected from Geological Survey of India (GSI), and Landsat 8 images were used to prepare the NDWI map.

A Flood Inventory Map (FIM) is crucial for predicting future floods. It is usually created by compiling historical flood data and analyzing them with computational models. The accuracy of any future flood vulnerability assessment depends on the reliability of past flood records (Debnath et al. 2023). A flood inventory map consists of past flood locations. For the present study area, annual flood reports were analyzed, and 133 validation flood points were drawn based on flood-inundated locations of the past 30 years. The present study constructed the Ajay River basin FIM within the GIS environment.

Analytic Hierarchy Process

Step 1: The Analytic Hierarchy Process (AHP) comparison matrix is a square shape matrix, where diagonal values (representing each criterion's importance relative to itself) are always 1. The off-diagonal values represent the relative importance of each criterion to each other criterion. The importances are assigned as per the dominance scale (Table 2) proposed by Saaty (1980).

$$A = \begin{matrix} C_{11} & C_{12} & C_{13} \\ C_{21} & C_{22} & C_{23} \\ C_{31} & C_{32} & C_{33} \end{matrix} \quad (1)$$

Step 2: For each pairwise matrix, the values within each column were added together. The sum of each column was then represented by the following equation (Eq. 2):

$$C_{ij} = \sum_{i=1}^{n} C_{ij} \quad (2)$$

Step 3: The normalization of each column value, subsequent to the second equation, can be represented by the following equations (Eq. 3):

$$X_{IJ} = \frac{c_{ij}}{\sum_{i=1}^{n} C^i} = \begin{matrix} X_{11} & X_{12} & X_{13} \\ X_{21} & X_{22} & X_{23} \\ X_{31} & X_{32} & X_{33} \end{matrix} \quad (3)$$

Step 4: A priority vector was calculated by normalizing the criterion values and then dividing each normalized value by the sum of normalized values in its row (Eq. 4):

$$W_{ij} = \frac{\sum_{j=1}^{n} X_{ij}}{n} = \begin{matrix} W_{11} \\ W_{12} \\ W_{13} \end{matrix} \quad (4)$$

Step 5: Calculation of eigenvalue (λ_{max}) (Eq. 5).

$$\lambda_{max} = \sum_{i}^{n} CV_{ij} \quad (5)$$

Step 6: The Consistency Index (CI) (Eq. 6) is used to calculate the consistency of the pairwise comparison matrix, where λ_{max} defines the maximum eigenvalue.

$$CI = \frac{\lambda_{max} - \text{n}}{n - 1} \quad (6)$$

Step 7: The Random Index (RI) is used to measure the consistency of a pairwise comparison matrix. Table 3 displays the RI index values for the CI.

Step 8: The Consistency Ratio (CR) (Eq. 7) indicates the reliability of the pairwise comparison matrix judgments of an AHP model; the CR thresholds are determined as 0.05 for a 3*3 matrix, 0.08 for a 4*4 matrix and 0.1 for a matrix greater than 5*5. CR values below the threshold are considered consistent and vice versa.

$$CR = \frac{CI}{RI} \quad (7)$$

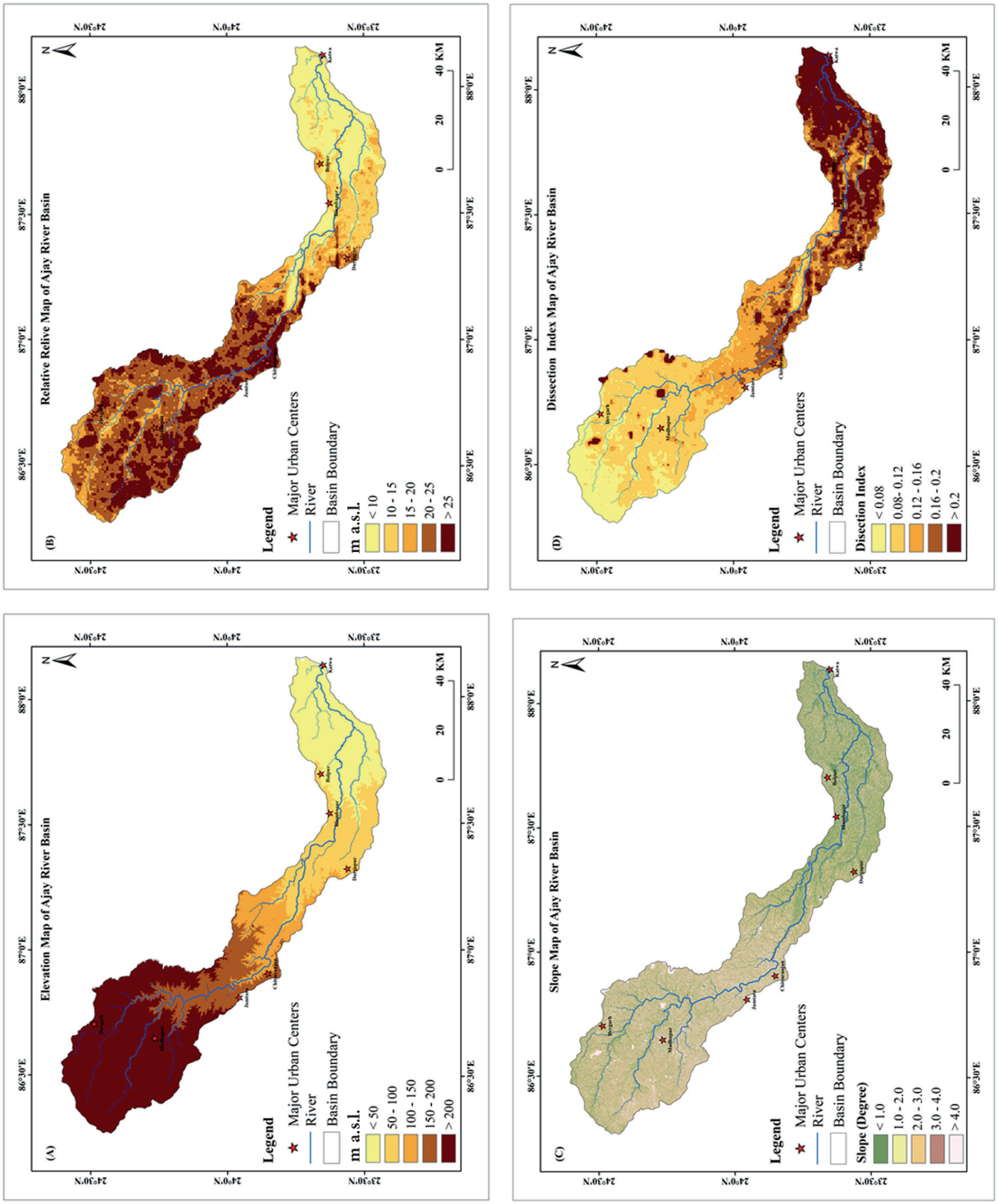

Fig. 3. Flood conditioning factors of the study: (A) Elevation, (B) Relative Relief, (C) Slope, (D) Dissection, (E) Ruggedness Index, (F) Length of Over land flow, (G) Drainage Density, (H) Drainage Frequency, (I) Drainage Texture, (J) NDWI, (K) Confluence Density, (L) Infiltration Number, (M) Soil Type, (N) Geology

Citation: Bulletin of Geography. Physical Geography Series 2025, 29, http://doi.org/10.12775/bgeo-2025-0009

Continuation of Figure 3

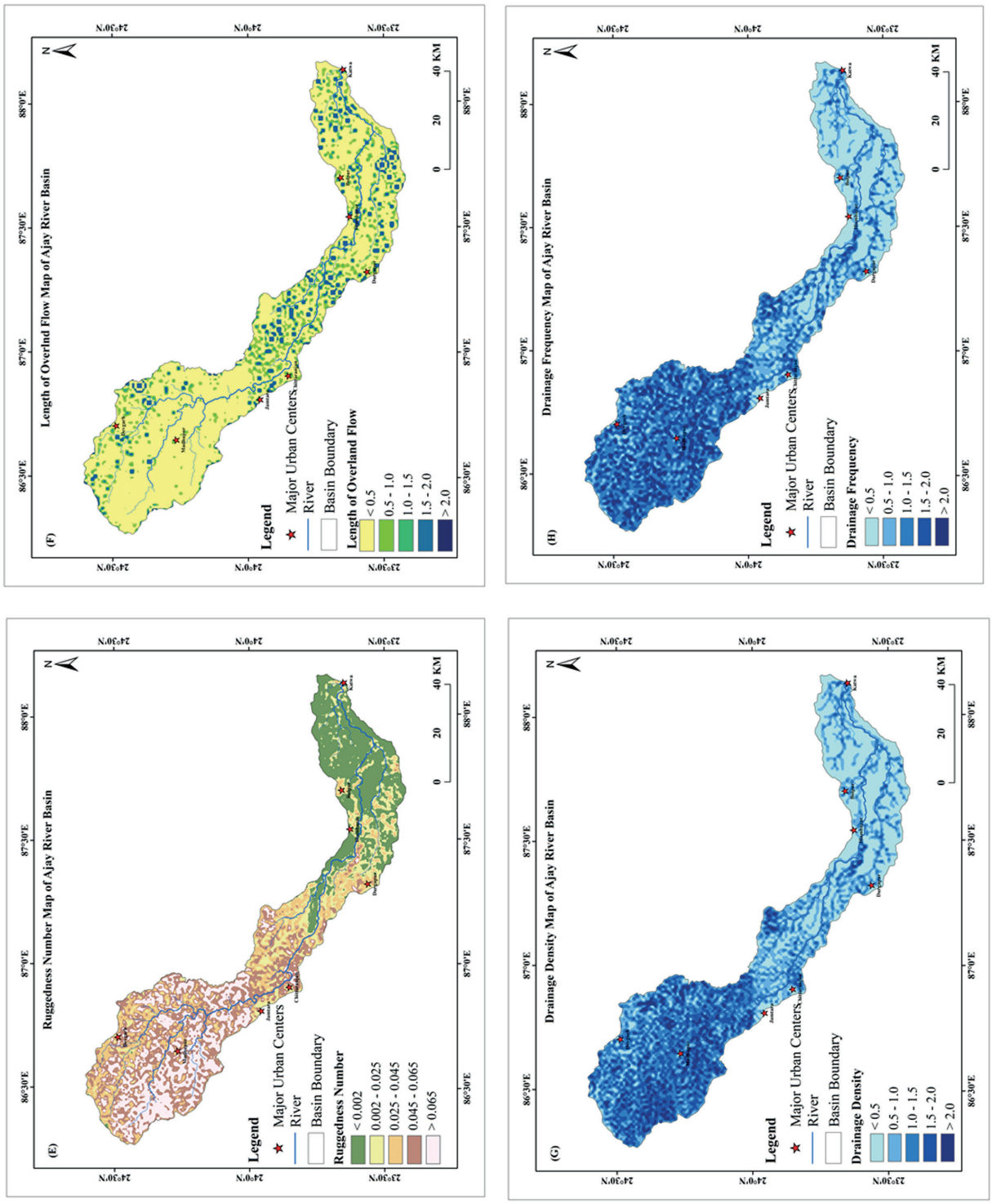

Continuation of Figure 3

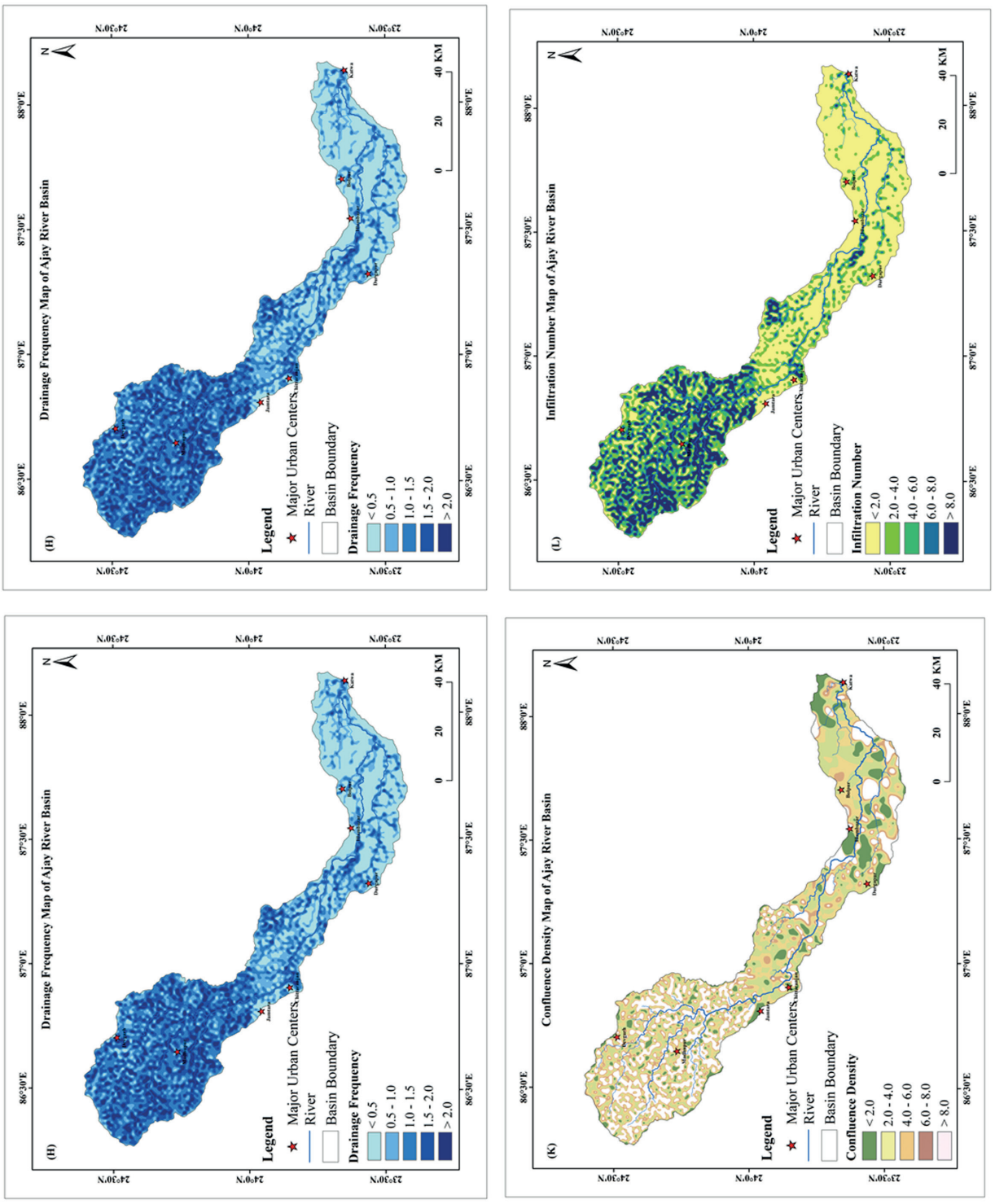

 Citation: Bulletin of Geography. Physical Geography Series 2025, 29, http://doi.org/10.12775/bgeo-2025-0009

Continuation of Figure 3

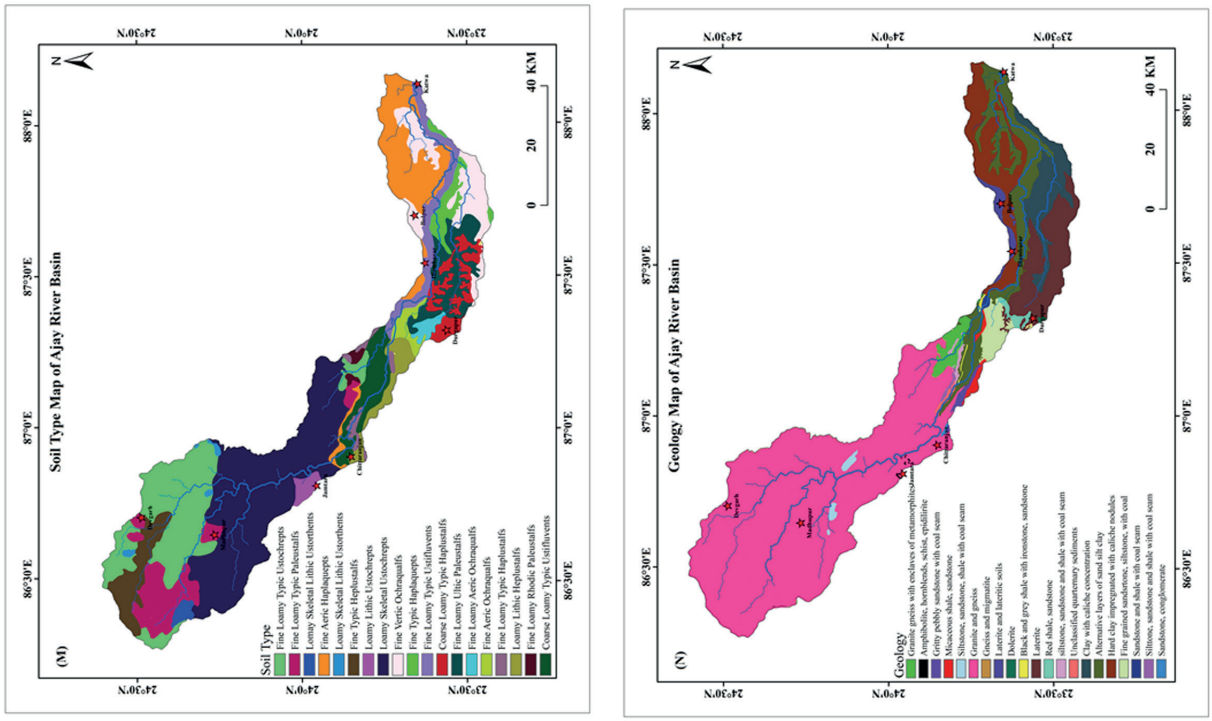

Table 1. All the considered flood conditioning factors (Beneficial, Non-beneficial)

Sl. No.	Beneficial Parameters	Non-Beneficial Parameters
1	Drainage Density	Elevation
2	Drainage Frequency	Relief
3	Drainage Texture	Dissection Index
4	NDWI	Ruggedness Number
5	Confluence Density	Slope
6	Soil Type	Length of Overland Flow
7	Geology	Infiltration Number

TOPSIS

The Technique for Order Preference and Similarity to Ideal Solution (TOPSIS) is a widely used multi-criterion decision-making tool developed by Yoon and Hwang in 1981 (Mitra and Das 2023). It employs a compensatory aggregation approach to determine the most suitable option among a set of alternatives. The method is based on the principle that the optimal alternative should be closest to the positive-ideal solution while being farthest from the negative-ideal solution.

Initially, alternatives are ranked based on their similarity to an ideal solution – a theoretical benchmark that represents optimal conditions in every aspect but may not be practically attainable; the higher an alternative's similarity to this ideal, the

Table 2. Description of scales for pairwise comparison Matrix (Source: Saaty 1980)

Scales	Degree of preferences	Descriptions
1	Equal importance	Two attributes with equally contribution to the objective
3	Moderate importance	Experience and judgment slightly favor one activity over another
5	Strong Importance	Experience and judgment strongly favor one activity over another
7	Very strong and Demonstrated Importance	An activity is favor very strongly favored over another, its dominance demonstrated in practice.
9	Extreme Importance	The evidence favoring one activity over another is the highest possible order of affirmation.
2,4,6,8	Intermediate values between adjacent scale values	When compromise is needed.

better its ranking. The TOPSIS approach involves calculating the distance of each alternative from the ideal solution and selecting the best option accordingly (Thakkar and Thakkar 2021).

Step 1: Decision matrix construction (Eq. 8):

$$D = x_{ij} \tag{8}$$

Step 2: Normalization of decision matrix: here, each decision matrix (x_{ij}) is divided by its norm (Eq. 9):

$$y_{ij} = \frac{x_{ij}}{\sqrt{\sum_{i=1}^{j} x_{ij}^2}} \; Where\ i = 1,2 \ldots\ldots I\ and\ j = 1,2, \ldots\ldots J \tag{9}$$

Step 3: Weightage integration in the normalized matrix: here, parameter weights are multiplied by the normalized matrix to form the weighted normalized matrix (Eq. 10).

$$v_{ij} = w_j * y_{ij}\ Where\ i = 1,2, \ldots\ldots I\ and\ j = 1,2, \ldots\ldots j \tag{10}$$

Step 4: Determination of ideal best (A^+) and ideal worst (A^-) solution based on the weighted normalized matrix (Eq. 11 & 12):

$$A^+ = \left(v_1^*, v_2^*, v_3^* \ldots\ldots\ldots v_j^*\right) \tag{11}$$

Where v_j*=max v_{ij} if j is a beneficial criterion or min v_{ij} if j is a non-beneficial criterion.

$$A^- = \left(v_j^-, v_1^-, v_3^- \ldots\ldots\ldots v_j^-\right) \tag{12}$$

Where v_j-= min v_{ij} if j is a beneficial criterion or max v_{ij} if j is a non-beneficial criterion.

Step 5: Separation value calculation from ideal positive and ideal negative solutions using the Euclidean distance method (eq. 13 & 14):

$$S^+ = \sqrt{\sum_{j-1}^{J} \left(v_{ij} - v_j^+\right)^2} \tag{13}$$

$$S^- = \sqrt{\sum_{j-1}^{J} \left(v_{ij} - v_j^-\right)^2} \tag{14}$$

Step 6: Calculation of relative closeness to ideal solution for obtaining overall performance score (Eq. 15):

$$p_i = \frac{S^-}{S^- + S^+} \tag{15}$$

VIKOR

The VIKOR (VIseKriterijumska Optimizacija I Kompromisno Resenje, meaning Multi-criterion Optimization and Compromise Solution) multi-criterion decision-making technique was first proposed by S. Opricovic in 1980 (Khosravi et al. 2019; Sari 2021; Mitra and Das 2023). The name VIKOR was adopted in 1990. This robust tool is applicable to a wide range of strategic decision-making problems across diverse fields, including social, economic and environmental contexts. The VIKOR approach involves identifying potential solutions (alternatives), determining their relative importance (priorities), ranking them accordingly, and ultimately selecting the best compromise solution based on this ranking (Thakkar & Thakkar 2021). Here, after the formation of the decision matrix, the ideal best and ideal worst values are chosen (Eq. 16 & 17).

$$A^+ = \max_j A_{ij}\ ,\ A^- = \min_j A_{ij}\ \text{for beneficial criteria}$$

Citation: Bulletin of Geography. Physical Geography Series 2025, 29, http://doi.org/10.12775/bgeo-2025-0009

Table 3. Random index value (Source: Saaty 1980)

N	1	2	3	4	5	6	7	8	9	10	11	12	13	14	15
RI	0.0	0.0	0.58	0.90	1.12	1.24	1.32	1.41	1.45	1.49	1.51	1.53	1.56	1.57	1.59

$A^+ = \min_j A_{ij}$, $A^- = \max_j A_{ij}$ for non-beneficial criteria

Sj, *Rj* and *Qj* values are computed following eq. 18, 19 and 20.

$$S_j = \sum_{i=1}^{j} w_j\left(A^+ - A_{ij}\right)/(A^+ - A^-)$$

$$R_j = \max_j \{w_j(A^+ - A_{ij})/(A^+ - A^-)\}$$

$$Q_j = v\left(S_j - S^+\right)/\left(S^- - S^+\right) + (1-v)(R_j - R^+)/(R^- - R^+)$$

Here, S^+ and R^+ represents the minimum value of S_j and R_j, respectively, and S^-, R^- defines the maximum value of the same. v defines the weight of strategy for S_j and R_j, which is 0.5. Q_j represents the final performance score of each points based on this point ranks were assigned, where the lowest value (Q_j) implies highest rank.

Receiver Operating Characteristic (AUC–ROC)

The Area Under the ROC Curve (AUC) is used to validate or examine the capability of a model to predict the probability of occurrence of hazards and disasters; ROC is the tradeoff between false positive and accurate positive rate along the X and Y axes (Pourghasemi et al. 2020). Its key aspects involve plotting the sensitivity, quantification of the successful and non-successful events, and 1-specificity on the abscissa and ordinates (Pourghasemi and Rahmati 2018; Malik et al. 2021). The value of the AUC curve varies between 0.5 to 1.0, a value between 0.9 and 1.0 indicates success or prediction rate, 0.8–0.9 indicates very good, 0.7–0.8 indicates good, 0.6–0.7 indicates moderate, and less than 0.6 indicates weak prediction rate of the model (Yesilnacar 2005; Chowdhury 2024).

Results and discussion

Functional Relation of Flood Conditioning Factors

The study considers different topographic, hydrological, drainage and river basin morphometric parameters (Table 1 and Fig. 3) to generate a flood-hazard map (FHM) of the Ajay River basin. Topographic factors influence flood occurrence by affecting water flow and accumulation. High absolute and relative reliefs, along with steep slopes, promote rapid runoff and potential flash floods. Low absolute and relative relief, coupled with gentle slopes, increases the risk of widespread inundation. A high ruggedness index creates complex flow patterns and concentrated runoff. The drainage parameters are more strongly positively correlated in flood occurrence by controlling water flow and accumulation. High drainage density, drainage frequency and fine drainage texture are efficient indicators of rapid runoff generation and water collection; simultaneously, confluence density shows the points or areas of stream junction where water volume increases, which commonly elevates downstream flood risk. The Normalized Difference Water Index (NDWI) indicates the presence of surface water, soil moisture and ground saturation. Generally, areas adjacent to rivers, lakes and other water bodies are highly saturated with moisture (having high NDWI), which makes this highly susceptible to flooding. The parameters like infiltration number and length of overland flow control surface runoff flow and infiltration capacity, as well as influencing flood occurrence. Low infiltration loss (low infiltration number), rapid channel expansion and water accumulation into river channels lead to rapid runoff generation, water accumulation and higher flood risk. Geology and soil are the significant factors influencing flood hazard; they control different aspects of flood occurrence like rock, soil properties, soil composition, porosity,

Table 4. Pair Wise Comparison Matrix

Parameters	Elevation	Relief	Slope	Dissection	Ruggedness	Infiltration number	Drainage Density	Drainage Frequency	Drainage Texture	NDWI	Confluence Density	LOF	Soil	Geology
Elevation	1.00	2.00	2.00	3.00	3.00	4.00	5.00	5.00	6.00	6.00	7.00	7.00	8.00	9.00
Relief	0.50	1.00	2.00	3.00	4.00	5.00	6.00	6.00	6.00	7.00	8.00	8.00	8.00	9.00
Slope	0.50	0.50	1.00	4.00	5.00	6.00	6.00	6.00	6.00	7.00	8.00	9.00	9.00	9.00
Dissection	0.33	0.33	0.25	1.00	2.00	3.00	3.00	3.00	3.00	5.00	6.00	7.00	8.00	9.00
Ruggedness	0.33	0.33	0.20	0.50	1.00	5.00	5.00	5.00	5.00	7.00	8.00	8.00	8.00	9.00
Infiltration number	0.25	0.20	0.17	0.33	0.20	1.00	3.00	3.00	3.00	4.00	5.00	6.00	7.00	8.00
Drainage Density	0.20	0.17	0.17	0.33	0.20	0.33	1.00	2.00	2.00	3.00	5.00	6.00	7.00	8.00
Drainage Frequency	0.20	0.17	0.17	0.33	0.20	0.33	0.50	1.00	2.00	3.00	4.00	5.00	6.00	7.00
Drainage Texture	0.17	0.17	0.17	0.33	0.20	0.33	0.50	0.50	1.00	3.00	4.00	5.00	6.00	7.00
NDWI	0.17	0.14	0.14	0.20	0.14	0.25	0.33	0.33	0.33	1.00	3.00	4.00	5.00	6.00
Confluence Density	0.14	0.13	0.13	0.17	0.13	0.20	0.20	0.25	0.25	0.33	1.00	3.00	4.00	5.00
LOF	0.14	0.13	0.11	0.14	0.13	0.17	0.17	0.20	0.20	0.25	0.33	1.00	2.00	3.00
Soil	0.13	0.13	0.11	0.13	0.13	0.14	0.14	0.17	0.17	0.20	0.25	0.50	1.00	3.00
Geology	0.11	0.11	0.11	0.11	0.11	0.13	0.13	0.14	0.14	0.17	0.20	0.33	0.33	1.00
Sum	4.2	5.5	6.7	13.6	16.4	25.9	31.0	32.6	35.1	47.0	59.8	69.8	79.3	93.0

Table 5. Normalized Matrix

Parameters	Elevation	Relief	Slope	Dissection	Ruggedness	Infiltration number	Drainage density	Drainage frequency	Drainage texture	NDWI	Confluence density	LOF	Soil	Geology	Criteria Weightage (CW)
Elevation	0.240	0.364	0.298	0.221	0.183	0.155	0.161	0.153	0.171	0.128	0.117	0.100	0.101	0.097	0.178
Relief	0.120	0.182	0.298	0.221	0.243	0.193	0.194	0.184	0.171	0.149	0.134	0.115	0.101	0.097	0.171
Slope	0.120	0.091	0.149	0.295	0.304	0.232	0.194	0.184	0.171	0.149	0.134	0.129	0.113	0.097	0.169
Dissection	0.080	0.061	0.037	0.074	0.122	0.116	0.097	0.092	0.085	0.106	0.100	0.100	0.101	0.097	0.091
Ruggedness	0.080	0.061	0.030	0.037	0.061	0.193	0.161	0.153	0.142	0.149	0.134	0.115	0.101	0.097	0.108
Infiltration number	0.060	0.036	0.025	0.025	0.012	0.039	0.097	0.092	0.085	0.085	0.084	0.086	0.088	0.086	0.064
Drainage Density	0.048	0.030	0.025	0.025	0.012	0.013	0.032	0.061	0.057	0.064	0.084	0.086	0.088	0.086	0.051
Drainage Frequency	0.048	0.030	0.025	0.025	0.012	0.013	0.016	0.031	0.057	0.064	0.067	0.072	0.076	0.075	0.044
Drainage Texture	0.040	0.030	0.025	0.025	0.012	0.013	0.016	0.015	0.028	0.064	0.067	0.072	0.076	0.075	0.040
NDWI	0.040	0.026	0.021	0.015	0.009	0.010	0.011	0.010	0.009	0.021	0.050	0.057	0.063	0.065	0.029
Confluence Density	0.034	0.023	0.019	0.012	0.008	0.008	0.006	0.008	0.007	0.007	0.017	0.043	0.050	0.054	0.021
LOF	0.034	0.023	0.017	0.011	0.008	0.006	0.005	0.006	0.006	0.005	0.006	0.014	0.025	0.032	0.014
Soil	0.030	0.023	0.017	0.009	0.008	0.006	0.005	0.005	0.005	0.004	0.004	0.007	0.013	0.032	0.012
Geology	0.027	0.020	0.017	0.008	0.007	0.005	0.004	0.004	0.004	0.004	0.003	0.005	0.004	0.011	0.009
Sum	1.000	1.000	1.000	1.000	1.000	1.000	1.000	1.000	1.000	1.000	1.000	1.000	1.000	1.000	1.000

Table 6. Model Decision matrix and Parameter Weightages

Sample Points	Elevation	Relief	Slope	Dissection	Ruggedness	Infiltration number	Drainage Density	Drainage Frequency	Drainage Texture	NDWI	Confluence Density	Length of Overland Flow	Soil	Geology
Weight	0.178	0.171	0.169	0.091	0.108	0.064	0.051	0.044	0.040	0.029	0.021	0.014	0.012	0.009
P1	5	2	1	1	3	3	5	4	3	2	3	1	1	1
P2	5	3	3	1	4	5	5	5	5	1	5	1	1	1
P3	5	4	3	1	5	4	5	5	3	1	3	1	1	1
P4	5	2	2	1	4	5	5	5	4	1	5	1	1	1
P5	5	3	1	1	4	3	5	4	3	1	2	1	1	1
P6	5	3	3	1	3	3	5	5	3	1	3	1	1	1
P7	5	4	1	1	3	1	2	2	2	1	2	2	1	1
P8	5	3	3	1	2	2	2	5	4	1	3	1	1	1
P9	5	3	2	1	2	1	2	5	3	1	3	2	1	1
P10	5	3	1	1	2	1	1	1	1	1	3	1	1	1
P6184	1	2	1	5	2	1	3	3	2	1	3	1	1	1
P6185	1	1	1	3	2	2	4	4	3	1	3	1	1	1
P6186	1	2	2	5	2	1	1	3	2	1	2	5	1	2
P6187	2	2	5	5	1	1	1	1	1	3	5	1	1	1
P6188	1	1	4	5	1	1	1	1	1	2	3	1	1	2
P6189	1	1	1	2	2	1	3	2	2	1	3	1	1	2
P6190	1	2	1	5	1	1	1	1	1	1	2	1	1	1
P6191	1	1	1	4	1	1	1	1	1	2	1	2	1	1
P6192	1	2	4	4	1	1	1	1	1	2	1	1	1	1
P6193	1	1	5	4	1	1	1	1	1	2	1	1	1	1

Citation: Bulletin of Geography, Physical Geography Series 2025, 29, http://doi.org/10.12775/bgeo-2025-0009

Table 7. Calculates final computation and interpolation matrix

Sample Points	TOPSIS			VIKOR		
	Si+	Si-	Pi	Si	Ri	Qi
P1	0.003	0.004	0.569	0.467	0.196	0.744
P2	0.004	0.003	0.395	0.640	0.196	0.854
P3	0.004	0.002	0.340	0.725	0.196	0.908
P4	0.004	0.003	0.453	0.556	0.196	0.801
P5	0.004	0.003	0.420	0.557	0.196	0.802
P6	0.004	0.003	0.420	0.607	0.196	0.833
P7	0.004	0.002	0.398	0.611	0.196	0.836
P8	0.004	0.003	0.443	0.589	0.196	0.822
P9	0.003	0.003	0.465	0.540	0.196	0.791
P10	0.003	0.003	0.459	0.559	0.196	0.803
P6410	0.001	0.004	0.797	0.175	0.047	0.115
P6411	0.001	0.005	0.818	0.159	0.045	0.101
P6412	0.001	0.004	0.740	0.259	0.047	0.169
P6413	0.003	0.004	0.542	0.397	0.182	0.660
P6414	0.003	0.005	0.650	0.276	0.137	0.448
P6415	0.001	0.005	0.769	0.206	0.068	0.198
P6416	0.001	0.004	0.778	0.202	0.047	0.132
P6417	0.001	0.017	0.939	0.173	0.046	0.110
P6418	0.003	0.004	0.623	0.354	0.137	0.497
P6419	0.003	0.005	0.590	0.352	0.182	0.632

permeability, landform evolution, drainage pattern, valley, flood plain development of the study area.

The above discussion portrays the functional relation of Flood-Conditioning Factors (FCFs). The Ajay River originates from the Chotanagpur Plateau in Bihar. It then enters Jharkhand, which accounts for more than half of its basin. The remaining portion of the basin lies within West Bengal, which topographically includes both the plateau fringe and alluvial plains. The basin portrays different types of topographic, hydrologic, drainage and environmental setups based on the geographic location. The upper catchment is characterized by high elevation, relief, rugged topography, high drainage properties, low soil moisture (low NDWI) and high infiltration number; simultaneously, the lower Ajay River basin belongs to the floodplain of the Ajay River with low elevated, relief, gentle slope surface, with high soil moisture content (high NDWI), alluvial sediment composed lithology – all these geographical characteristics make the region highly flood-hazard-prone. Analytic Hierarchy Process (AHP) was used to rank the parameters and assign weightage. As outlined in Table 5 and Figure 4; elevation (0.178), relief (0.171) and slope (0.169) are the most significant factors, carrying highest weightage. These are followed by dissection index (0.091), ruggedness index (0.108), infiltration number (0.064), drainage density (0.051) and drainage frequency (0.044). Soil and geology have the least influence, with weightings of 0.012 and 0.009.

Decision matrix for the models

The flood hazard maps were developed using fourteen FCFs. They represent geomorphology, geology, topography, drainage, infiltration, soil type and morphometric characteristics of the Ajay River basin. Since analysis of both the utilized models, i.e. TOPSIS and VIKOR, is based on a pixel approach, the initial decision matrix for the fourteen FCFs was extracted from 6,193 points. Initially, the Ajay River basin was divided into 1-km² grids, and one point was drawn for each grid. Based on the function characteristics, flood inducing capacity and literature review, seven parameters each were classified to the beneficial and non-beneficial categories. Assigning

weightages to the parameters is an important step in MCDM models; here, the weightages were calculated using the Analytic Hierarchy Process.

Computation and Interpolation of the indices

Tables 6 and 7 represent point-wise computational and interpolation values (Pi, Qi) of each model; in the TOPSIS model, the S+ TOPSIS values range from 0.005 to 0.001, and S- TOPSIS values range from 0.017 to 0.002. To interpolate the final TOPSIS FHM, the Pi value was utilized, which varies from 0.939 to 0.0.281. Conversely, the VOKOR model employees the Si and Ri value to calculate the Qi value, which is further utilized to interpolate the final VIKOR FHM. The Si and Ri values range from 0.872 to 0.091 and 0.191 to 0.027, respectively, and the final Qi value varies between 1.00 and 0.002.

Flood Hazard Map Assessment

All the drawn flood hazard maps are systematically classified into five classes, i.e. very high, high, moderate, low and very low. The very high and high values indicate higher flood hazard probability, and vice versa. As mentioned in Figure 5, both FHMs, i.e. TOPSIS and VIKOR, delineated 1479.45 and 1387.21 km², respectively, as being in the very high or high flood hazard categories. This indicates that both FHMs consistently identified the same region as falling into the very high flood hazard zone, comprising approximately 35% of the total Ajay River basin area. Also, the spatial distributions of the hazard zones are remarkably similar among all the FHMs. The Ajay River basin extends through three different states, originating in Bihar and then passing through Jharkhand and onwards to West Bengal. Areas in Bihar and Jharkhand belong to low and very low flood-hazard zones; on the other hand, the entire West Bengal part belongs to very high and high flood-hazard classes. This part comprises of Purba Bardhaman, Paschim Bardhaman and Birbhum Districts and includes major settlements like Bolpur-Shantiniketan and Katwa, as well as parts of Durgapur, Chittaranjan, Dubrajpur, Seuri, etc.

Model validation

The final risk maps were evaluated through a comparative analysis using predefined validation points obtained from the flood inventory map. The AUC–ROC curve (Fig. 7) was applied for

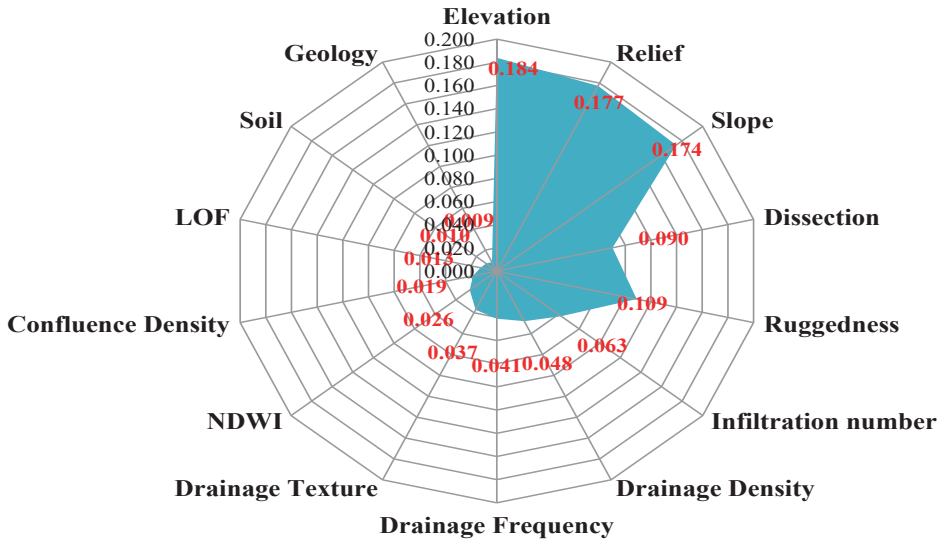

Fig. 4. Radar diagram showing the weightages of the flood conditioning factors

Citation: Bulletin of Geography. Physical Geography Series 2025, 29, http://doi.org/10.12775/bgeo-2025-0009

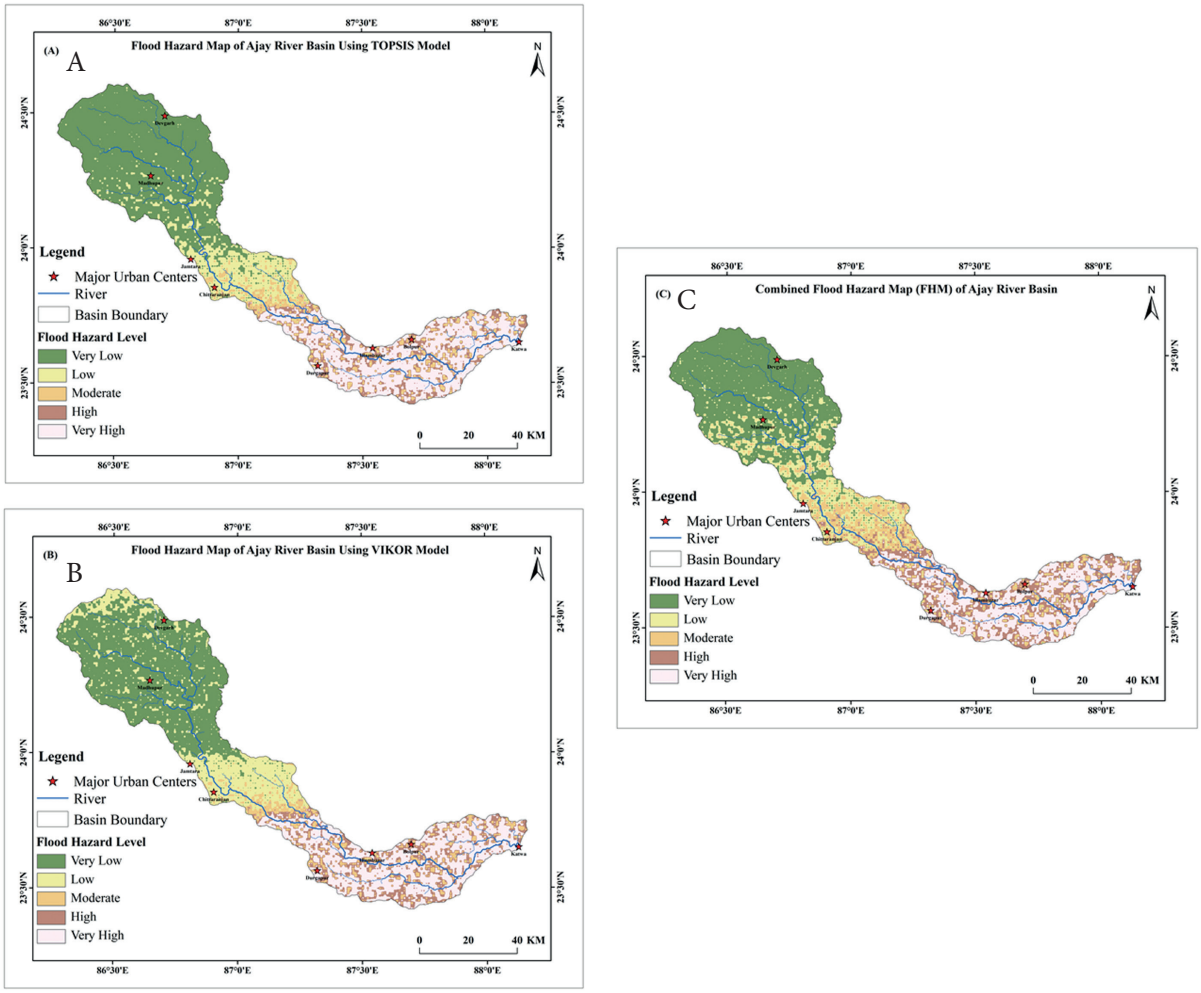

Fig. 5. Final flood hazard map: (A) TOPSIS, (B) VIKOR (C) Combines

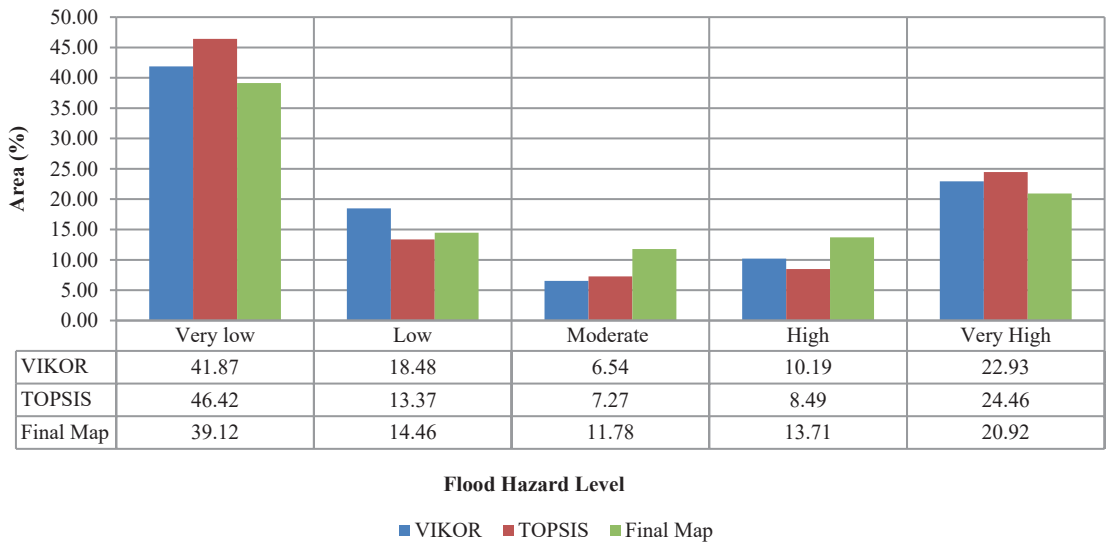

	Very low	Low	Moderate	High	Very High
VIKOR	41.87	18.48	6.54	10.19	22.93
TOPSIS	46.42	13.37	7.27	8.49	24.46
Final Map	39.12	14.46	11.78	13.71	20.92

Fig. 6. Bar diagram representing area distribution of the generated flood hazard maps

model validation, resulting in AUC values of 0.827 for TOPSIS and 0.837 for VIKOR. According to the classification scale, AUC values above 0.9 are considered excellent, while those exceeding 0.8 are rated as very good. These findings affirm the reliability and effectiveness of these models in accurately generating flood susceptibility maps.

Discussion

The study delineates flood hazard zones in the Ajay River basin using 14 flood-controlling factors which represent the geomorphic, topographic, drainage, geologic and soil properties of the study area. Parameter weightages were assigned using a knowledge-based subjective AHP model. The parameters were ranked based on a review of scientific flood literature relating to the study area, researcher knowledge and the physical setup of the study area. Elevation (0.178), relief (0.171) and slope (0.169) are the most influential factors in the study area, having the highest weightages. Low-elevated topography, gentle slope, high topographic wetness and accumulation of monsoonal rainfall make a region susceptible to flooding. As shown in Fig. 5, areas downstream of Padaveswar are highly and very highly flood-hazard-prone. As mentioned by the previous studies, the extent of flood inundation suddenly extends towards the right bank downstream of Illambazar and from Bolpur it spreads widely along both the banks. Downstream of Satkahonia, the frequency of flood occurrence also increases at the gauging stations at Maliara, Gheropara and Natunhat; downstream of Pandaveswar, the average slope of the basin decreases significantly (Mukhopadhyay 2010; Roy 2012). According to annual flood reports, the water level of Ajay River at Gheropara Gauging Station reaches Dangerous Level (DL) and Extremely Dangerous Levels (EDL) during the monsoon season. Specifically, the water level reached 41.8 meters on September 30, 2021; 37.9 meters on September 30, 2019; 37.18 meters on July 26, 2017; 38.42 meters on August 12, 2016; and 38.1 meters on July 4, 2014. Several villages were affected by these floods. In 2021, the affected villages included Rosui, Billeswar, and Chorki Bortala (under Billeswar G.P., Ketugram-II Block, Purba Bardhaman), and Sundarpur, Thupsara (Nanoor Block, Birbhum). The 2022 floods impacted Gheedaha, Jhasra (Bolpur-Sriniketan Block) and Mouza Begunkola (Ketugram-II Block). In 2023, the floods affected Panchoa Bahiri/Itanda (Bolpur-Santiniketan Block), Tupsara/Kargram (Nanoor Block), and Pandugram/Charki (Ketugram-II Block). These floods caused significant damage, amounting to Rs. 12,074,000 in 2023, Rs. 6,526,000 in 2022 and Rs. 314,541,000 in 2021.

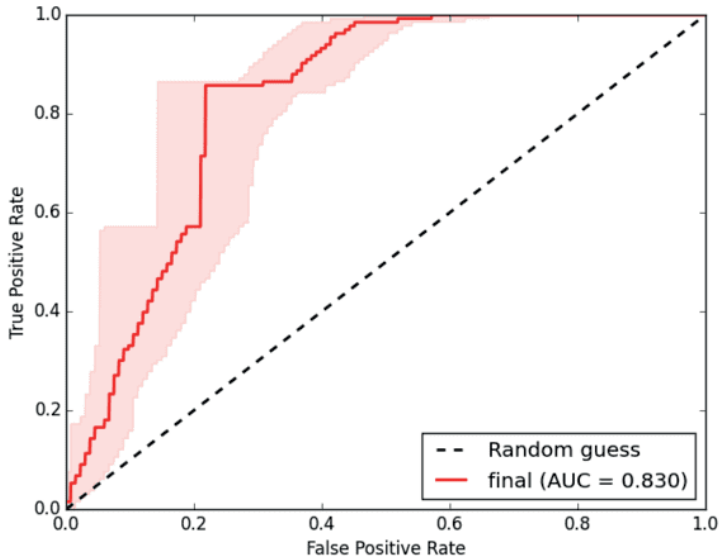

Fig. 7. ROC curve showing accuracy of the generated flood hazard maps

Citation: Bulletin of Geography. Physical Geography Series 2025, 29, http://doi.org/10.12775/bgeo-2025-0009

The final flood hazard map indicates that 35% (Fig. 6) of the basin area is highly flood-hazard prone. The entire area is located within the lower Ajay River basin, which spans three districts, i.e. Paschim Bardhaman, Purba Bardhaman and Birbhum, with a total collective population of more than 2.5 million (approximate) and a high population density (Barddhaman: 1,099 person per km2 and Birbhum: 771 person per km2). Several major urban centers, like Bolpur, Katwa, Dugapur, Chittaranjan and Illambazar, are located within this section of the river, which also falls under the very high flood-hazard zones.

Conclusion

Flood remains a significant environmental hazard in the present study area; it calls for an intrinsic analysis of effective management strategies. The current study employs an intrinsic hybridization approach using MCDM models (viz. TOPSIS, VIKOR) to develop a flood-hazard map of the river basin. With the help of a geospatial tool, multiple thematic flood-triggering factors were integrated to produce the final flood-hazard map (FHM); five hazard zones (viz. very high, high, moderate, low and very low) were created based on the calculated flood-hazard index. The accuracy of the final FHM was validated using the receiver operating characteristics (AUC–ROC) method. This shows an AUC value of 0.83, which indicates good performance of the model. Instead of operating differences, all the models identified the lower Ajay River basin as highly and very highly susceptible to floods; in most cases, these classifications accompanied areas of low elevation, gentle slope, high soil moisture, wetness, high drainage density, high drainage frequency channel planform riparian, which occupy 35% of the total study area.

Several limitations remain in terms of spatial resolution variation among the influencing factors, the inability of any model to replicate real-world scenarios, and limited accessibility of geospatial datasets. Despite the limitations, these maps can serve as a useful tool for flood management stakeholders, such as policymakers, planners, engineers and local administration, and can provide empirical support in the region's strategic decision-making to target enhanced flood mitigation and management. The breaching of embankments, reduced channel carrying capacity, siltation, and narrower downstream channel width are some of the primary influencing factors of flood occurrence in the study area. The study suggests remedial measures including channel widening, increasing water-holding capacity, embankment maintenance and an advanced early-warning system as effective flood management measures in the study area. Further research can focus on hydrologic and hydrodynamic analysis using modeling approaches based on past flood data, which may provide deeper insight into flood inundation depth, extent and risk management in the study area.

Disclosure statement

No potential conflict of interest was reported by the authors.

Author contributions

Study design: CP; data collection: SG; statistical analysis: SG; manuscript preparation: CP; literature review: SG.

Acknowledgement

We are very much thankful to the Department of Geography, Assam University Diphu Campus (AUDC), Diphu, Karbi Anglong, Assam, India, 782462 for their support during this research. The authors acknowledge the funding support by University Grant Commission (UGC), India, to conduct the research, under the UGC-JRF fellowship.

References

ANTWI-AGYAKWA KT, AFENYO MK and ANGNUURENG DB, 2023, Know to predict, forecast to warn: a review of flood risk prediction tools. *Water* 15(3): 427. DOI: https://doi.org/10.3390/w15030427.

BANDYOPADHYAY S, KAR NS, DAS S and SEN J, 2014, River systems and water resources of West Bengal: a review. *Geological Society of India special publication* 3(2014): 63-84.

BRAUERS WK and ZAVADSKAS EK, 2006, The MOORA method and its application to privatization in a transition economy. *Control and cybernetics* 35(2): 445-469.

CHOWDHURY MS, 2024, Flash flood susceptibility mapping of north-east depression of Bangladesh using different GIS based bivariate statistical models. *Watershed Ecology and the Environment* 6: 26-40. DOI: https://doi.org/10.1016/j.wsee.2024.01.001.

DEBNATH J, SAHARIAH D, MAZUMDAR M, LAHON D, MERAJ G, HASHIMOTO S and others, 2023, Evaluating flood susceptibility in the brahmaputra river basin: an insight into Asia's Eastern Himalayan floodplains using machine learning and multi-criteria decision-making. *Earth Systems and Environment* 7(4): 733-760. DOI: https://doi.org/10.1007/s41748-023-00355-z.

DEVANAND MR and KUNDAPURA S, 2021, Flood inundation mapping of harangi river basin, kodagu, using GIS techniques and HEC-RAS model. *Trends in Civil Engineering and Challenges for Sustainability: Select Proceedings of CTCS 2019*: 665-678. DOI: https://doi.org/10.1007/978-981-15-6828-2_49.

DI BALDASSARRE G, MONTANARI A, LINS H, KOUTSOYIANNIS D, BRANDIMARTE L and BLÖSCHL G, 2010, Flood fatalities in Africa: from diagnosis to mitigation. *Geophysical research letters* 37(22). DOI: https://doi.org/10.1029/2010GL045467.

DUAN Y, 2024, *Global projections of flood risk under climate change (No. EGU24-7030)*. Copernicus Meetings.

DUAN Y, XIONG J, CHENG W, LI Y, WANG N, SHEN G and YANG J, 2022, Increasing global flood risk in 2005–2020 from a multi-scale perspective. *Remote Sensing* 14(21): 5551. DOI: https://doi.org/10.3390/rs14215551.

GHORABAEE MK, AMIRI M, SADAGHIANI JS and ZAVADSKAS EK, 2015, Multi-criteria project selection using an extended VIKOR method with interval type-2 fuzzy sets. *International Journal of Information Technology & Decision Making* 14(05): 993-1016. DOI: https://doi.org/10.1142/S021962201550023X.

GHORABAEE MK, AMIRI M, ZAVADSKAS EK, TURSKIS Z and ANTUCHEVICIENE J, 2017, A new multi-criteria model based on interval type-2 fuzzy sets and EDAS method for supplier evaluation and order allocation with environmental considerations. *Computers & Industrial Engineering* 112: 156-174. DOI: https://doi.org/10.1016/j.cie.2017.08.017.

GLAS H, ROCABADO I, HUYSENTRUYT S, MAROY E, SALAZAR CORTEZ D, COOREVITS K and others, 2019, Flood risk mapping worldwide: A flexible methodology and toolbox. *Water* 11(11): 2371. DOI: https://doi.org/10.3390/w11112371.

GUPTA L and DIXIT J, 2022, A GIS-based flood risk mapping of Assam, India, using the MCDA-AHP approach at the regional and administrative level. *Geocarto International* 37(26): 11867-11899. DOI: https://doi.org/10.1080/10106049.2022.2060312.

KADER Z, ISLAM MR, AZIZ MT, HOSSAIN MM, ISLAM MR, MIAH M and JAAFAR WZW, 2024, GIS and AHP-based flood susceptibility mapping: a case study of Bangladesh. *Sustainable Water Resources Management* 10(5): 170. DOI: https://doi.org/10.1007/s40899-024-01081-8.

KHOSRAVI K, SHAHABI H, PHAM BT, ADAMOWSKI J, SHIRZADI A, PRADHAN B and PRAKASH I, 2019, A comparative assessment of flood susceptibility modeling using multi-criteria decision-making analysis and machine learning methods. *Journal of Hydrology* 573: 311-323. DOI: https://doi.org/10.1016/j.jhydrol.2019.03.073.

MALIK S, PAL SC, ARABAMERI A, CHOWDHURI I, SAHA A, CHAKRABORTTY R and others, 2021, GIS-based statistical model for the prediction of flood hazard susceptibility. *Environment, Development and Sustainability* 23: 16713-16743. DOI: https://doi.org/10.1007/s10668-021-01375-3.

MITRA R and DAS J, 2023, A comparative assessment of flood susceptibility modelling of GIS-based TOPSIS, VIKOR, and EDAS techniques in the Sub-Himalayan foothills region of Eastern India. *Environmental Science and Pollution Research* 30(6):

16036-16067. DOI: https://doi.org/10.1007/s11356-022-23167-6.

MITRA R, SAHA P and DAS J, 2022, Assessment of the performance of GIS-based analytical hierarchical process (AHP) approach for flood modelling in Uttar Dinajpur district of West Bengal, India. *Geomatics, Natural Hazards and Risk* 13(1): 2183-2226. DOI: https://doi.org/10.1080/19475705.2022.2112094.

POURGHASEMI HR and RAHMATI O, 2018, Prediction of the landslide susceptibility: Which algorithm, which precision? *Catena* 162: 177-192. DOI: https://doi.org/10.1016/j.catena.2017.11.022.

POURGHASEMI HR, KARIMINEJAD N, AMIRI M, EDALAT M, ZARAFSHAR M, BLASCHKE T and CERDA A, 2020, Assessing and mapping multi-hazard risk susceptibility using a machine learning technique. *Scientific reports* 10(1): 3203. DOI: https://doi.org/10.1038/s41598-020-60191-3.

PRASOJO OA, HURST MD, WILLIAMS RD, NAYLOR LA and TONEY J, 2024, Slowing down the tidal flood wave is the key to reducing tidal flood risk in estuaries worldwide (No. EGU24-17737). Copernicus Meetings.

ROY S, 2012, Spatial Variation of Floods in the Lower Ajay River Basin, West Bengal: A Geo-Hydrological Analysis. *International Journal of Remote Sensing and GIS* 1(2): 132-143.

SARKAR D and MONDAL P, 2020, Flood vulnerability mapping using frequency ratio (FR) model: a case study on Kulik river basin, Indo-Bangladesh Barind region. *Applied Water Science* 10(1): 1-13. DOI: https://doi.org/10.1007/s13201-019-1102-x.

SHAH AI and PAN ND, 2024, Flood susceptibility assessment of Jhelum River Basin: A comparative study of TOPSIS, VIKOR and EDAS methods. *Geosystems and Geoenvironment* 3(4): 100304. DOI: https://doi.org/10.1016/j.geogeo.2024.100304.

THAKKAR JJ and THAKKAR JJ, 2021, Technique for order preference and similarity to ideal solution (TOPSIS). *Multi-Criteria Decision Making*: 83-91. DOI: https://doi.org/10.1007/978-981-33-4745-8_8.

VASHIST K and SINGH KK, 2024, Flood hazard mapping using GIS-based AHP approach for Krishna River basin. *Hydrological Processes* 38(6): e15212. DOI: https://doi.org/10.1002/hyp.15212.

YESILNACAR EK, 2005, *The application of computational intelligence to landslide susceptibility mapping in Turkey*. University of Melbourne, Department.

ZHRAN M, GHANEM K, TARIQ A, ALSHEHRI F, JIN S, DAS J and others, 2024, Exploring a GIS-based analytic hierarchy process for spatial flood risk assessment in Egypt: a case study of the Damietta branch. *Environmental Sciences Europe* 36(1): 1-25. DOI: https://doi.org/10.1186/s12302-024-00936-3.

Received 21 April 2025
Accepted 15 July 2025